

# Automated Placement of Individual Millimeter-Wave Wall-Mounted Base Stations for Line-of-Sight Coverage of Outdoor Urban Areas

Sebastian S. Szyszkowicz, *Member, IEEE*, Andrés Lou, and Halim Yanikomeroglu, *Senior Member, IEEE*

**Abstract**—In this letter, advanced concepts in polygon computational geometry are combined to automate the placement of thousands of millimeter-wave (mmWave) wall-mounted base stations over two large urban areas, and to gather their line-of-sight coverage statistics; this is the first large-scale fully-automated channel modeling study of mmWave cells over massive open building data. This allows for a more accurate modeling of small-cell mmWave access networks, which are currently considered as a strong candidate technology for providing gigabit rates to dense urban areas.

**Index Terms**—Channel modeling, line-of-sight, cell planning, millimeter-wave, computational geometry.

## I. INTRODUCTION

**S**MALL cells and millimeter wave (mmWave) carriers (> 20 GHz) are currently considered as some of the most viable technologies for providing gigabit mobile access in dense urban centres [1]–[3]. These high expected rates are due to a combination of very wide (multi-GHz) available bandwidths [2], [4] and low expected interference [2]. Indeed, the systems are expected to be noise-limited, due to a combination of the aforementioned high bandwidth, and strong dynamic interference mitigation through directional beamforming with massive MIMO [2], [4], [5]. However, urban mmWave measurements in Manhattan [4] show that their propagation is strongly bounded by the line-of-sight (LOS) condition [1], [2], [4], resulting in low outdoor-to-indoor penetration and non-LOS coverage, while LOS links allow for good communication over distances of up to about 200 m, which is now often the assumed radius of these small cells [2]–[5]. These characteristics make mmWaves ideal for small-cell LOS outdoor urban coverage.

The small cell size, combined with the LOS condition, makes the propagation strongly dependent on the layout of the buildings in the urban area, and some recent mmWave system studies consider using small 2D urban maps [3], or random [5] or regular [2] rectangular buildings to model the LOS coverage areas more realistically. Some studies at lower frequencies (2.4 GHz),

where the LOS condition is also quite important [Sec. 1.3.1] [6], also use site-specific maps [7], [8].

Meanwhile, recent years have seen the advent of massive open map data [9], which allows for studies over much larger areas [10]. In order to progress from small localized propagation studies on open maps [11] to large-scale studies, it is necessary to intelligently process the maps so as to place fixed base stations in reasonable locations, as this can no longer be done manually. One work [7] places 2.4 GHz base stations automatically on top of buildings using an advanced ray-tracing and optimization tool. Still, most works on automated placement of fixed base stations only consider distances and propagation channels [12]–[15], and, in one case, topographical data [16], but not the shapes of buildings.

In this letter, we develop an algorithm to place below-rooftop wall-mounted base stations (WMBSs) automatically using a simpler propagation model (the LOS area), more appropriate for mmWave carriers. In [2] mmWave base stations are manually placed on street intersections of a small map; we propose that identifying urban features (such as intersections) on maps with highly-irregular buildings can be automated using computational geometry [17]–[20].

## II. PHYSICAL SETUP

The WMBS is defined by its placement on an outer vertical building facade, so as to provide an access link to mobile stations in the streets and open areas below. In the dense centre of a European city such as Paris, France, the roofline and the land topography are relatively flat, thus a WMBS's coverage area can be studied based on 2D building shapes.

The WMBS is backhauled either by wire [2] into the building, or wirelessly (as a relay): to a larger base station located above the roofline [12], [21], and/or in a multihop/mesh manner with other similar stations [2], [12]. The building also provides a wired power source opportunity.

We don't specify a height for the WMBS, but recommend the highest possible in normal cases, as it is most likely to maximize both the over-roofline wireless backhaul opportunities (e.g., in Central Paris [21]), and avoid most low-level obstacles (people, vehicles, kiosks, etc.) in the access link (though high tree foliage may be a counterexample to this).

The next section formulates the problem of finding good 2D locations for WMBSs as a computational geometry problem.

## III. GEOMETRICAL PROBLEM FORMULATION

The WMBS placement problem is formulated and solved in terms of computational geometry, with concepts and quantities summarized in Table I. The primitive object in our computational geometry problem will be the simple polygon (SP); it is

Manuscript received December 15, 2015; accepted March 30, 2016. Date of publication April 8, 2016; date of current version June 17, 2016. This work was supported in part by the National Sciences and Engineering Research Council (NSERC) of Canada and in part by TELUS Corporation. The associate editor coordinating the review of this paper and approving it for publication was A. Bletsas.

S. S. Szyszkowicz and H. Yanikomeroglu are with the Department of Systems and Computer Engineering, Carleton University, Ottawa, ON K1S-5B6, Canada (e-mail: sz@sce.carleton.ca; halim@sce.carleton.ca).

A. Lou was with the School of Electrical Engineering and Computer Science, University of Ottawa, Ottawa, ON, Canada. He is now with the Department of Computer Science, Concordia University, Montreal, QC, Canada, and also with the Department of Linguistics, Concordia University, Montreal, QC, Canada.

Digital Object Identifier 10.1109/LWC.2016.2552168

TABLE I  
COMPUTATIONAL GEOMETRY NOTATION AND OBJECTS

SP	Simple Polygon
VP	Visibility Polygon (LOS region)
GVD	Generalized Voronoi Diagram (of a set of SPs)
NN	Nearest Neighbour (on a GVD)
$r$	Cell radius: taken as 200 m in many mmWave system studies
$b_k$	2D building shape (SP)
$B_i$	2D block shape (SP)
$\mathcal{B}$	Set of all blocks $B_i$
$V(\mathcal{B}, \mathbf{p}, r)$	VP seen from point $\mathbf{p}$ to a maximum distance $r$ with obstacles $\mathcal{B}$
$\mathcal{O}_i$	Set of candidate WMBS locations $\mathbf{p}_{i,j}$ on the facade of block $B_i$
$C_i$	GVD cell associated with $B_i$ of a GVD partition of $\mathcal{B}$
$\ell_{i,j}$	NN link: shortest segment connecting two NN blocks $B_i$ and $B_j$
$N_i$	Number of NNs of block $B_i$
$\{\mathcal{P}_{i,j}\}_{j=1}^{N_i}$	Partition of contour of $B_i$ according to contact points with $\{\ell_{i,j}\}_{j=1}^{N_i}$ (See Fig. 2)

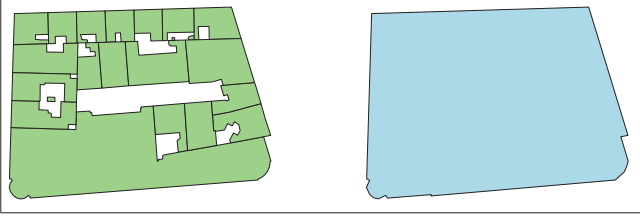


Fig. 1. Example of how adjacent buildings (left) are merged into a block, with inside holes removed (right), using the polygonal union operation [22].

defined as an area bounded by a closed non-self-touching path of line segments. A 2D building  $b_k$  is thus naturally represented by an SP, where each straight wall is represented by a segment. A 2D building database is thus a set of SPs  $\{b_k\}$ , many of which touch. We group the adjacent buildings into city blocks  $B_i$  using the polygonal union operation [22], and remove the inside holes (courtyards), as done in [10] and shown in Fig. 1. This results in a city map  $\mathcal{B} = \{B_i\}$ , which is a set of SPs  $B_i$  that are disjoint by construction.

The geometrical problem is: given a set  $\mathcal{B} = \{B_i\}$  of disjoint blocks, for a given  $B_i$ , find a set of candidate WMBS locations  $\mathcal{O}_i = \{\mathbf{p}_{i,j}\}$  on the contour of  $B_i$  such that the LOS region viewed from each  $\mathbf{p}_{i,j}$  has a locally maximum area. A formalization of this “local maximum”, and a computational geometry solution, are proposed in the next section.

#### IV. WMBS LOCATION CANDIDATE ALGORITHM

##### A. Generalized Voronoi Diagram and Natural Neighbours

In a regular grid of city blocks, it is trivial to identify neighbouring blocks, as they have a simple order. In a real city, blocks have irregular shapes, locations, and sizes; to bring order to such a complex environment, we take inspiration from approaches in intelligent motion planning around polygonal obstacles: for a set  $\mathcal{B}$  of disjoint SPs, the generalized Voronoi diagram (GVD) [17], [18] associates a GVD cell  $C_i$  to each SP  $B_i$  in  $\mathcal{B}$ , so that that each point in  $C_i$  is closer to  $B_i$  than to any other SP in  $\mathcal{B}$ . Then, any two SPs  $B_i$  and  $B_j$  in  $\mathcal{B}$  are said to be natural neighbours (NNs) if their GVD cells touch. Then, if  $B_i$  and  $B_j$  are NNs, one can define their “NN link”, which is the shortest segment  $\ell_{i,j}$  that connects  $B_i$  to  $B_j$ .

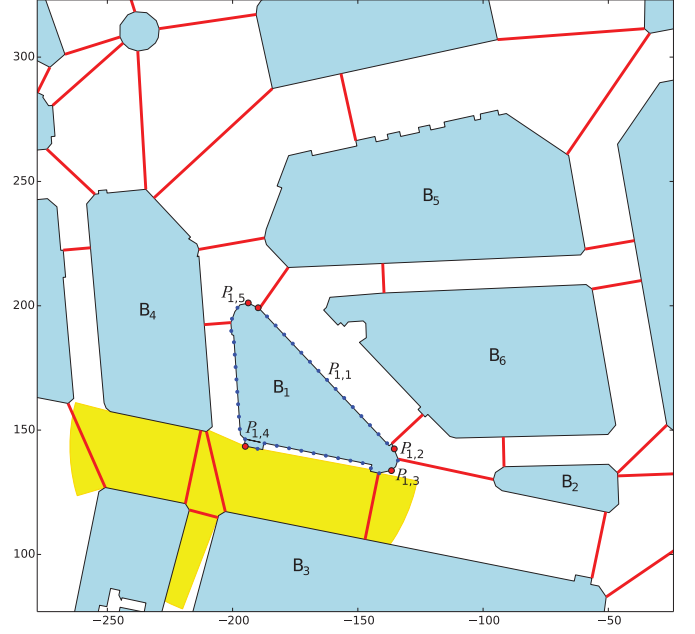


Fig. 2. Searching for optimal placements of WMBSs on the exterior of block  $B_1$ . Blocks are shown as shaded polygons; NN links are shown as thick red lines; search points  $\mathbf{p}$  are shown as blue dots (the spacing is exaggerated for illustration).  $B_1$  has five NNs  $B_2, \dots, B_6$ ; the NN links partition the contour of  $B_1$  into five regions:  $\mathcal{P}_{1,1}, \dots, \mathcal{P}_{1,5}$ . In each of the five regions, one locally-optimal WMBS location (given  $r = 50$  m) is shown (large red dot). The LOS region of one of the location solutions is shown (yellow polygon).

An SP  $B_i$  has  $N_i$  NNs, and thus  $N_i$  contact points between itself and each of its  $N_i$  NN links: These contact points partition the contour of  $B_i$  into  $N_i$  regions  $\mathcal{P}_{i,1}, \dots, \mathcal{P}_{i,N_i}$ , as seen in Fig. 2. Each of these partitions is defined by two consecutive NNs, and thus forms a natural region in which to search for an intersection. NN links thus give a systematic and natural way of defining regions  $\mathcal{P}_{i,j}$  for finding locally optimal locations on the contour of  $B_i$ .

##### B. Visibility Polygon

The Visibility Polygon (VP) is well-known ongoing research problem in computational geometry, with many algorithms available for its evaluation [19], [20]. The VP requires a “set of polygonal holes” (in our case, the set  $\mathcal{B}$  of disjoint blocks), a “guard” or “observer” point  $\mathbf{p}$ , and (optionally) a maximal radius  $r > 0$ . The VP  $V$  is the set of all points  $\mathbf{s}_i$  that verify:

- 1) the segment  $\overline{\mathbf{s}_i\mathbf{p}}$  does not cross (but may touch)  $\mathcal{B}$ , and
- 2)  $\|\overline{\mathbf{s}_i\mathbf{p}}\| \leq r$ .

The VP  $V(\mathcal{B}, \mathbf{p}, r)$  thus represents the LOS region seen from point  $\mathbf{p}$  to a maximum distance  $r$ , with a set of obstacles  $\mathcal{B}$ .

##### C. Proposed Algorithm

Our WMBS placement algorithm uses the VP and NN links geometric computations, and searches<sup>1</sup> along the walls of a block  $B_i$  for the LOS region with the highest area along each

<sup>1</sup>In practice, there are two implementation issues in this search: 1) One must quantize the continuous line  $\mathcal{P}_{i,j}$  into a discrete set of nearby points so that a sequential search can be performed, and 2) Because the search points are exactly on the contour of  $B_i$ , some VP algorithms may be confused as to which side is the interior of the polygon. One way to circumvent this problem is to move the search point away from  $B_i$  by a small amount.

wall section  $\mathcal{P}_{i,j}$  delimited by two consecutive NN links, thus looking for intersections or open areas (plazas, etc.) when possible (see Fig. 2).

---

#### WMBS CANDIDATE PLACEMENT ALGORITHM

**Require:** a set of disjoint SPs  $\mathcal{B}$ ; one block  $B_i$  and its partition  $\mathcal{P}_{i,1}, \dots, \mathcal{P}_{i,N_i}$  according to its  $N_i$  NN links;  $r > 0$ .  
**Ensure:**  $\mathcal{O}_i$  a set of WMBS candidate locations on  $B_i$ .  
 $\mathcal{O}_i \leftarrow$  empty set of points.  
**for**  $j = 1, \dots, N_i$  **do**  
  **for**  $\mathbf{p}$  in  $\mathcal{P}_{i,j}$  **do**  
    Find the area of the LOS region  $V(\mathcal{B}, \mathbf{p}, r)$   
  **end for**  
   $\mathbf{p}_{\max} \leftarrow \mathbf{p}$  that maximizes the area of  $V$ .  
  Add  $\mathbf{p}_{\max}$  to  $\mathcal{O}_i$ .  
**end for**  
**return**  $\mathcal{O}_i$ .

---

In the next section, we run this algorithm over a large number of urban maps, and summarize the statistics of the resulting LOS coverage areas.

#### V. PERFORMANCE ON REAL CITY MAPS

Maps of 2D buildings are taken from the OpenStreetMap project [9]–[11]. Massive open city data, combined with our algorithm, enables a fully automated study of WMBS LOS coverage over a large urban area. We consider two such areas: South Manhattan Island (NY, USA) and Central Paris (France). We divide each area into  $1 \text{ km} \times 1 \text{ km}$  tiles, displaced 500 m from each other (so that there is overlap), and consider “dense tiles” that are at least 40% covered by  $\mathcal{B}$ , and have each of their four quadrants at least 45% covered by  $\mathcal{B}$ , so as to avoid major open areas and large bodies of water<sup>2</sup>. WMBSs are placed according to the algorithm from Section IV, with a LOS radius of  $r = 200 \text{ m}$ , on all blocks located entirely within the inner  $600 \text{ m} \times 600 \text{ m}$  area, i.e.,  $r = 200 \text{ m}$  away from each edge, so as to avoid edge effects. An example from each urban area is shown in Figs. 3 and 4. We observe that the algorithm tends to place WMBSs on block corners and intersections; as long as  $r$  is greater than about 100 m (roughly the typical block size), the WMBSs locations will be similar.

The cumulative distribution functions (CDFs) of the LOS areas of typical WMBSs are shown in Fig. 5 as a fraction of the total circular area within a link distance of  $R = 50, 100, 150, 200 \text{ m}$ , and their means ( $\hat{\mu}$ ) and standard deviations ( $\hat{\sigma}$ ) are given in Table II. These LOS coverage results can be used together with pathloss models to calculate link budgets and rate coverage for outdoor urban areas.

The shapes of the resulting cells are highly irregular, as observed in [3, Fig. 3] and [5, Fig. 2a)], usually “star-shaped”, and in significant contrast to the more-or-less circular mmWave cells described in [23]. For Manhattan, the 11.3% LOS coverage area of a circle of radius 200 m is consistent with the 11% area given in [3] for the same radius and urban area. The LOS

<sup>2</sup>The choice of the values (40,45)% was found by trial-and-error and visual inspection of all resulting maps. It was found to be a quick way to select dense tiles and makes our results easy to reproduce.



Fig. 3. WMBSs candidate locations (red dots) on a  $1 \text{ km}^2$  tile of Manhattan Island, NY (centre:  $73.9909^\circ \text{W}$ ,  $40.7373^\circ \text{N}$ ), with  $r = 200 \text{ m}$ . We manually select a few of the candidate locations (green dots) and show their LOS regions (in yellow) to illustrate what typical LOS coverage regions may look like.

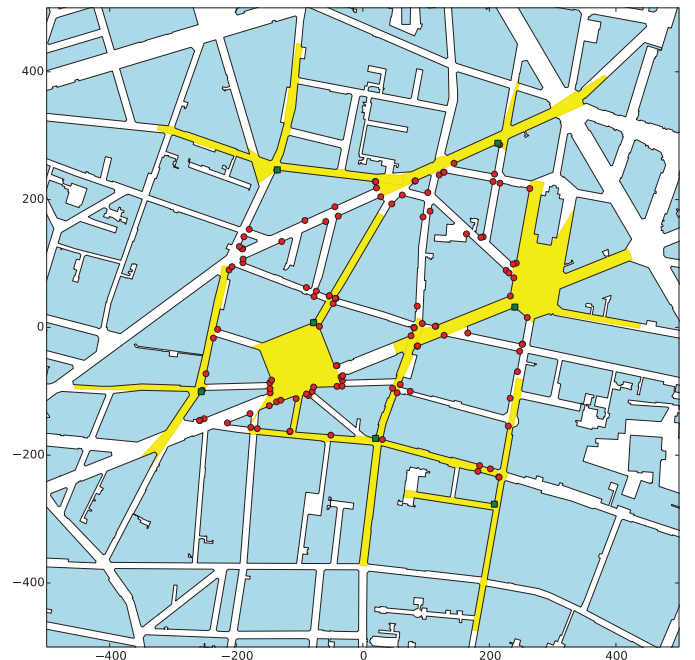


Fig. 4. WMBSs candidate locations (red dots) on a  $1 \text{ km}^2$  tile of Central Paris, France (centre:  $2.3479^\circ \text{E}$ ,  $48.8774^\circ \text{N}$ ), with  $r = 200 \text{ m}$ . We manually select a few of the candidate locations (green dots) and show their LOS regions (in yellow) to illustrate what typical LOS coverage regions may look like.

coverage is about 20% lower in Paris for all radii, due to the narrower, more irregular, streets. This shows how the nature of the street layout affects the deployment of wall-mounted LOS cells, and their coverage areas.

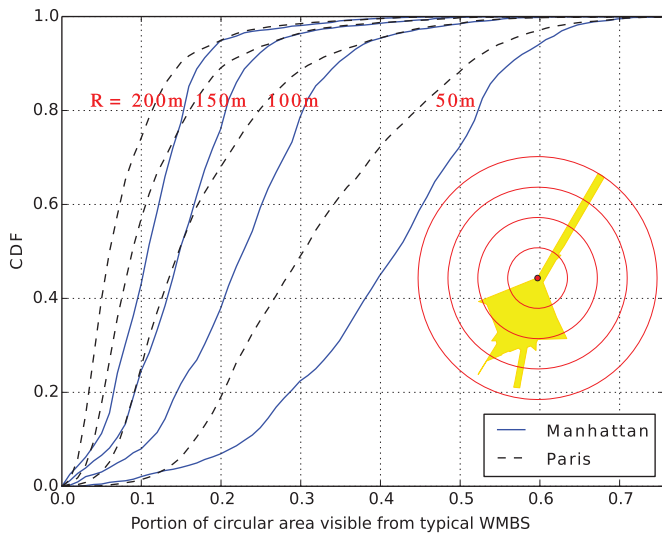


Fig. 5. Distribution functions of fraction of LOS area within circles of radii  $R = 50, 100, 150,$  and  $200$  (with one LOS region shown for illustration, with the corresponding circles). WMBSs are placed based on the setup given in Table II with  $r = 200$  m. Naturally, the LOS portion can rarely exceed 75%, since each WMBS requires at least a building corner to be mounted on.

TABLE II  
SIMULATION SETUP AND RESULTS SUMMARY

Urban Area	South Manhattan	Central Paris
Centre	73.9939°W 40.7373°N	2.3343°E 48.8594°N
Area Size	3.5 km × 6 km	10 km × 8 km
Tiles	6 × 11	19 × 15
Dense Tiles	29	88
WMBSs placed	4172	12309
LOS area within:		
50 m	$\hat{\mu} = 40.6\%, \hat{\sigma} = 13.3\%$	$\hat{\mu} = 32.3\%, \hat{\sigma} = 13\%$
100 m	$\hat{\mu} = 22.3\%, \hat{\sigma} = 9.9\%$	$\hat{\mu} = 17.5\%, \hat{\sigma} = 10\%$
150 m	$\hat{\mu} = 15.3\%, \hat{\sigma} = 7.6\%$	$\hat{\mu} = 11.2\%, \hat{\sigma} = 8.0\%$
200 m	$\hat{\mu} = 11.3\%, \hat{\sigma} = 6.1\%$	$\hat{\mu} = 7.87\%, \hat{\sigma} = 6.2\%$

## VI. CONCLUSION AND FUTURE WORK

This work demonstrates how two computational geometry concepts, natural neighbours and visibility polygons, can be used to place mmWave cells automatically on a city map.

Future work may include an algorithm for finding small subsets of the candidate locations found here that can provide good coverage to a city area, as well as augmenting the LOS regions with good non-LOS regions for better coverage estimation.

The automation of the placement of small cell locations, combined with the massive open geographical data, makes it possible to automate very large propagation and system simulations on real world maps, making such large simulations more and more accessible to the average researcher.

## REFERENCES

- [1] J. Andrews *et al.*, "What will 5G be?" *IEEE J. Sel. Areas Commun.*, vol. 32, no. 6, pp. 1065–1082, Jun. 2014.
- [2] M. Abouelseoud and G. Charlton, "System level performance of millimeter-wave access link for outdoor coverage," in *Proc. IEEE Wireless Commun. Netw. Conf. (WCNC)*, Apr. 2013, pp. 4146–4151.
- [3] S. Singh, M. Kulkarni, A. Ghosh, and J. Andrews, "Tractable model for rate in self-backhauled millimeter wave cellular networks," *IEEE J. Sel. Areas Commun.*, vol. 33, no. 10, pp. 2196–2211, Oct. 2015.

- [4] T. Rappaport *et al.*, "Millimeter wave mobile communications for 5G cellular: It will work!" *IEEE Access*, vol. 1, pp. 335–349, May 2013.
- [5] T. Bai and R. Heath, "Coverage and rate analysis for millimeter-wave cellular networks," *IEEE Trans. Wireless Commun.*, vol. 14, no. 2, pp. 1100–1114, Feb. 2015.
- [6] "Guidelines for evaluation of radio interface technologies for IMT-advanced," Tech. Rep. ITU-R M.2135-1, Dec. 2009 [Online]. Available: [https://www.itu.int/dms\\_pub/itu-r/opb/rep/R-REP-M.2135-1-2009-PDF-E.pdf](https://www.itu.int/dms_pub/itu-r/opb/rep/R-REP-M.2135-1-2009-PDF-E.pdf).
- [7] M. Deruyck, W. Joseph, and L. Martens, "Power consumption model for macrocell and microcell base stations," *Trans. Emerging Telecommun. Technol.*, vol. 25, no. 3, pp. 320–333, 2014.
- [8] S. Savazzi, R. H. de Souza, and L. B. Becker, "System level performance of millimeter-wave access link for outdoor coverage," in *Proc. Wireless Netw. Planning Optim. Oil Gas Refineries*, Dec. 2013, pp. 29–34.
- [9] S. Sehra, J. Singh, and H. Rai, "A systematic study of OpenStreetMap data quality assessment," in *Proc. Int. Conf. Inf. Technol. New Gener. (ITNG)*, Apr. 2014, pp. 377–381.
- [10] M. Mirahsan, R. Schoenen, S. Szyszkowicz, and H. Yanikomeroglu, "Measuring the spatial heterogeneity of outdoor users in wireless cellular networks based on open urban maps," in *Proc. IEEE Int. Conf. Commun. (ICC)*, Jun. 2015, pp. 2834–2838.
- [11] J. Nuckelt, D. Rose, T. Jansen, and T. Kurner, "On the use of OpenStreetMap data for V2X channel modeling in urban scenarios," in *Proc. 7th Eur. Conf. Antennas Propag. (EuCAP)*, Apr. 2013, pp. 3984–3988.
- [12] A. So and B. Liang, "Optimal placement and channel assignment of relay stations in heterogeneous wireless mesh networks by modified Bender's decomposition," *Elsevier Ad Hoc Netw.*, vol. 7, no. 1, pp. 118–135, Jan. 2009.
- [13] S. Wang, W. Zhao, and C. Wang, "Approximation algorithms for cellular networks planning with relay nodes," in *Proc. IEEE Wireless Commun. Netw. Conf. (WCNC)*, Apr. 2013, pp. 3230–3235.
- [14] W. Guo and T. O'Farrell, "Relay deployment in cellular networks: Planning and optimization," *IEEE J. Sel. Areas Commun.*, vol. 31, no. 8, pp. 1597–1606, Aug. 2013.
- [15] O. Bulakci, J. Hamalainen, and E. Schulz, "Performance of coarse relay site planning in composite fading/shadowing environments," in *Proc. IEEE 24th Int. Symp. Pers. Indoor Mobile Radio Commun. (PIMRC)*, Sep. 2013, pp. 2689–2694.
- [16] W. Guo, S. Wang, X. Chu, J. Zhang, J. Chen, and H. Song, "Automated small-cell deployment for heterogeneous cellular networks," *IEEE Commun. Mag.*, vol. 51, no. 5, pp. 46–53, May 2013.
- [17] R. Bonfiglioli, W. van Toll, and R. Geraerts, "GPGPU-accelerated construction of high-resolution generalized Voronoi diagrams and navigation meshes," in *Proc. Int. Conf. Motion Games*, Nov. 2014, vol. 7, pp. 25–30.
- [18] D. Kuan, J. Zamiska, and R. Brooks, "Natural decomposition of free space for path planning," in *Proc. IEEE Int. Conf. Robot. Autom.*, Mar. 1985, vol. 2, pp. 168–173.
- [19] S. Ghosh, *Visibility Algorithms in the Plane*. Cambridge, U.K.: Cambridge Univ. Press, 2007.
- [20] F. Bungiu, M. Hemmer, J. Hershberger, K. Huang, and A. Kröller, "Efficient computation of visibility polygons," in *Proc. Eur. Workshop Comput. Geometry (EuroCG)*, Mar. 2014, pp. 1–4.
- [21] "Planning non-line-of-sight wireless backhaul networks," *SIRADEL and BLiNQ Networks*, Tech. Rep., 2012 [Online]. Available: <http://www.slideshare.net/frankrayal/planning-non-lineof-sight-wireless-backhaul-networks>.
- [22] F. Martínez, A. J. Rueda, and F. R. Feito, "A new algorithm for computing Boolean operations on polygons," *Comput. Geosci.*, vol. 35, no. 6, pp. 1177–1185, 2009.
- [23] A. Nassar, A. Sulyman, and A. Alsanie, "Achievable RF coverage and system capacity using millimeter wave cellular technologies in 5G networks," in *Proc. IEEE 27th Can. Conf. Elect. Comput. Eng. (CCECE)*, May 2014, pp. 1–6.